Adult neural stem cells in distinct microdomains generate previously unknown interneuron types

Published in final edited form as:
Nat Neurosci. 2014 February ; 17(2): 207–214. doi:10.1038/nn.3610.

Adult neural stem cells in distinct microdomains generate previously unknown interneuron types

Florian T. Merkle[1,2,3,+], **Luis C. Fuentealba**[1,+], **Timothy A. Sanders**[1], **Lorenza Magno**[4], **Nicoletta Kessaris**[4,#], and **Arturo Alvarez-Buylla**[1,#,*]

[1]Department of Neurological Surgery, and the Eli and Edythe Broad Center of Regeneration, Medicine and Stem Cell Research, University of California, San Francisco, California 94143, USA

[2]Harvard Stem Cell Institute, Harvard University, Cambridge, MA 02138, USA

[3]Departments of Molecular and Cellular Biology, and Stem Cell and Regenerative Biology, Harvard University, Cambridge, MA 02138, USA

[4]Wolfson Institute for Biomedical Research and Department of Cell and Developmental Biology, University College London, Gower Street, London WC1E 6BT, UK

Abstract

Throughout life, neural stem cells (NSCs) in different domains of the ventricular-subventricular zone (V-SVZ) of the adult rodent brain generate several subtypes of interneurons that regulate the function of the olfactory bulb (OB). The full extent of diversity among adult NSCs and their progeny is not known. Here, we report the generation of at least four previously unknown OB interneuron subtypes that are produced in finely patterned progenitor domains in the anterior ventral V-SVZ of both the neonatal and adult brain. Progenitors of these novel interneurons are responsive to sonic hedgehog (SHH) and are organized into microdomains that correlate with the expression domains of the Nkx6.2 and Zic family of transcription factors. This work reveals an unexpected degree of complexity in the specification and patterning of NSCs in the postnatal mouse brain.

INTRODUCTION

The mammalian ventricular-subventricular zone (V-SVZ) is a powerful model system for studying the processes of neurogenesis, migration, and functional integration of newborn neurons. Each day, neural stem cells (NSCs) in the rodent V-SVZ produce thousands of interneurons that migrate to the olfactory bulb (OB), the brain region where olfactory information is first processed[1]. Continual interneuron turnover is essential for the maintenance of OB structure and olfactory discrimination[1–3].

*To whom correspondence should be addressed: abuylla@stemcell.ucsf.edu.
+These authors contributed equally to this work
#senior authors

Author contributions

F.T.M., L.C.F., and A.A.B. conceived and designed the experiments. F.T.M., L.C.F., T.A.S., and L.M. conducted experiments. N.K. developed the *Nkx6.2CreER*^{T2} transgenic mice and critically reviewed and edited the manuscript. F.T.M., L.C.F., and A.A.B. analyzed data and prepared the manuscript. F.T.M wrote the manuscript.

Neurons derived from the postnatal V-SVZ mature into OB periglomerular cells (PGCs) or granule cells (GCs). PGCs can be further subdivided into three non-overlapping subtypes based on the expression of calbindin, calretinin, and tyrosine hydroxylase (CalB+, CalR+, and TH+, respectively) [4]. GCs can be subdivided into four subtypes based on the location of their cell bodies in the intermediate (G_I), deep (G_{II}), or superficial (G_{III}) layers of the granule cell layer (GCL), and their expression of CalR[5]. Each postnatally born neuron subtype plays a distinct role in the OB circuitry[6]. Our understanding of the full diversity of postnatally-born interneuron types is incomplete, hampering efforts to understand the functional role of adult neurogenesis.

Adult-born OB neurons are produced by astrocyte-like NSCs (B1 cells) in the V-SVZ[7] an extensive germinal zone lining the postnatal lateral ventricle on its lateral wall and portions of its medial wall, extending rostrally towards the OB core and dorsally and caudally into the subcallosal zone (reviewed in reference 8). Recently, it has been recognized that different types of interneurons are produced in different sub-regions of the postnatal V-SVZ[9–12]. Defining the borders of these progenitor domains and identifying the cell types produced from each domain is a critical first step towards understanding the molecular mechanisms underlying neuronal subtype specification in the adult brain.

To explore the extent of diversity among NSCs and the cell types they produce, we mapped NSC progenitor domains in the newborn V-SVZ. We discovered new progenitor domains in the lateral ventricle that produce four previously unknown subtypes of postnatally-born OB interneurons in both the newborn and adult brain. These cell types are generated from narrow microdomains patterned by the Nkx6.2 and Zic family of transcription factors (TFs), suggesting a functional role for these TFs in adult neurogenesis. The wide variety of cell types produced in such a small region highlights and extends the utility of the postnatal V-SVZ as a model system for studying the molecular mechanisms of neuronal subtype specification.

RESULTS

Identification of novel OB interneuron subtypes

The spatial origin of different OB interneuron types has been studied by tracing the lineage of NSCs expressing regionally restricted TFs. However, since TF expression domains tend to be large and there is a limited repertoire of Cre mice that can be used for lineage tracing studies, this approach has limited power to uncover new stem cell populations. To complement TF-based lineage tracing, we previously developed a lineage tracing technique that takes advantage of the uniquely long basal process of radial glia, the principal NSC in embryonic and early postnatal brains (reviewed in reference 13). These basal processes are readily infected by adenoviruses, which are then retrogradely transported to the radial glial cell body. Since adenoviral diffusion in the brain parenchyma is limited, this technique results in the infection of a small, spatially restricted patch of NSCs in the V-SVZ[9]. When an adenovirus expressing Cre recombinase (Ad:Cre) is injected into reporter mice that express GFP upon Cre-mediated recombination (Z/EG)[14], infected cells and their progeny become permanently labeled with GFP.

In this study, we labeled radial glial cells by injecting small volumes (20 nl) of Ad:Cre into the brains of neonatal (P0) Z/EG mice and analyzed their progeny in the OB 28 days later by morphology and immunostaining for cell-type-specific markers. We targeted NSCs throughout the V-SVZ, including the subcallosal zone[15], dorsal[16] and medial walls[9] of the lateral ventricle, and the RMS[17] (reviewed in reference 8). We observed labeled cells in the V-SVZ and the OB in 310 injected hemispheres. By varying the stereotaxic coordinates and angle of injection (Fig. 1a), we could reproducibly label different NSC populations along the medial and lateral walls of the lateral ventricle (Fig. 1b–d).

As previously reported, progenitors in the dorsal V-SVZ and subcallosal zone produced predominantly TH+ PGCs and superficial GCs[9,11], and the RMS yielded large proportions of PGCs relative to other labeled OB cell types[9]. The ventral V-SVZ produced CalB+ PGCs and deep GCs, as expected, but closer observation of brains containing anterior ventral V-SVZ labeling we observed interneurons with distinctive morphologies that we had not seen before. We studied the morphology of these cells in detail using immunoperoxidase staining for GFP, which resulted in the Golgi-like filling of their cell bodies and fine processes. We identified four novel interneuron subtypes with distinctive morphologies. The novel cell types had extensively branched dendritic arbors that frequently bore spines, characteristic of mature, functionally integrated neurons (Fig. 1e–i, 3, and S1). In particular, their dendritic arbors and small cell bodies (approximately 6–7 μm/8–9 μm minor/major axis diameter) resembled those of OB interneurons and a subset of them expressed the interneuron marker CalR (Fig. 3e, S1, and S2). We refer to these novel interneurons as Type 1-4 cells.

To determine whether these novel interneurons are also generated from adult neural stem cells, we stereotaxically injected Ad:GFAP-Cre into the ventral V-SVZ of P60 Z/EG mice. Ad:GFAP-Cre is an adenovirus that expresses Cre in GFAP+ cells, so infected GFAP+ cells and their progeny are specifically and permanently labeled in Cre reporter mice[9,18]. Upon Ad:GFAP-Cre injection, labeled cells in the V-SVZ were confined to the medial and lateral walls of the ventral tip of the V-SVZ (Fig. 2a,b). 28 days after viral injection, we observed Type 1-4 cells in 10 injected hemispheres that targeted the ventral V-SVZ (Fig. 2c–f) but not in 32 hemispheres in which the dorsal V-SVZ was targeted. We conclude that Type 1-4 cells are generated in the adult ventral V-SVZ by GFAP+ progenitors.

Characterization of Type 1-4 cells

To further characterize Type 1-4 cells, we examined their expression of known neurochemical markers. We did not observe any Type 1-4 cells that expressed TH, somatostatin, parvalbumin or CalB. However, a significant fraction of each cell type expressed CalR (Fig. 3 and S2). The finding that Type 1-4 cells are CalB− but CalR+ confirms that these cells are distinct from the CalB+ PGCs produced in the ventral V-SVZ[9,16].

Type 1 cells resembled GCs, but were clearly distinct from previously characterized G_I, G_{II}, or G_{III} cells[19]., In stark contrast to superficial GCs (G_{III}) whose dendrites project near the top of the EPL, the dendrites of Type 1 cells frequently failed to reach beyond the internal plexiform layer (IPL). Furthermore, whereas the dendrites of G_I, G_{II}, or G_{III} cells branch primarily in the mitral cell layer and EPL, the dendrites of this cell type branched primarily

below the mitral cell layer in deeper regions of the OB (Fig. 1i, 3, and S1). Following the naming convention of Shepherd and Greer[6], we call these cells deep-branching granule cells (G_{IV}). Cells resembling deep-projecting granule cells have previously been observed in the hamster and rabbit olfactory bulbs[20,21] but were not known to be generated postnatally.

Type 2 cells resembled granule cells and had small, smooth cell bodies that lacked basal dendrites and were restricted to the mitral cell layer. These cells almost always extended only a single primary dendrite into the deep layer of the EPL. This dendrite branched extensively, giving rise to many small dendrites decorated with numerous spines-like protrusions, though their arbors were spatially confined (Fig. 1i, 3, and S1). Based on their distinctive shrub-like dendritic arbors, we call Type 2 cells shrub granule cells (G_V). Shrub cells have not been described in detail, but Blanes mentions “tiny granule cells of the mitral cell layer”[22] that could correspond to Type 2 cells.

The cell bodies of Type 3 cells were confined to the mitral cell layer, from which they extended multiple thin, mostly spineless processes that branched both below and above the mitral cell layer, and weaved torturously in the mitral cell layer and IPL rather than being directed to the EPL (Fig. 1i, 3, and S1). In some of these cells, immunoperoxidase staining revealed very lightly stained, fine processes extending straight up into the EPL that might correspond to axons. Since Type 3 cells are located in the mitral cell layer and have dendritic arbors confined to this region, we call them perimitral cells (PMC). Perimitral cells are distinct from horizontal or vertical short axon cells, which have significantly larger cell bodies (13–17 μm) and are usually found in the IPL[23].

Type 4 cells typically had cell bodies distributed throughout the EPL. To clearly distinguish them from Type 3 cells and PGCs, we limited our analysis to cells separated by at least 100 μm from both the mitral cell layer or glomerular layer. The dendrites of Type 4 cells were branched, largely confined to the EPL, often projected radially, and were decorated with varicosities but few spines (Fig. 1i, 3, and S1). We occasionally observed a fine, lightly stained process, presumably an axon, that exited the cell body laterally and bifurcated radially. We identify Type 4 neurons as satellite cells (SC) of the mouse main OB since they strongly resemble the satellite cells described in the main OB of hedgehogs[24] and the “dwarf” neurons of the rat accessory OB[25]. Satellite cells were clearly distinct from Van Gehuchten cells[26] (Fig. S2), which were PV+, had larger cell bodies (~13 μm), and were rarely seen following neonatal injections but never from adult injections.

GLI1$^+$ progenitors contribute to Type 1-4 cell generation

During embryogenesis, progenitor domains are set up by a combination of cell intrinsic and cell intrinsic factors acting on NSCs. V-SVZ progenitors likely maintain a cell-autonomous TF code, since they continue producing specific cell types when transplanted ectopically[9]. However, environmental factors may modulate this code since activation of the Sonic hedgehog (SHH) pathway is sufficient to partially re-specify superficial GCs to deep GCs[27]. Since the TF GLI1, a target gene of SHH, is highly expressed in the ventral V-SVZ, we hypothesized that SHH signaling in the ventral V-SVZ might contribute to Type 1-4 cell specification. We therefore made use of *Gli1::CreER^{T2};R26-Ai14* mice[28] to identify OB neurons generated from *Gli1*+ stem cells. In these mice, the *Gli1* promoter drives expression

of CreER^{T2}, which translocates to the nucleus in the presence of tamoxifen[29] and excises a STOP cassette, activating a tdTomato reporter gene (Fig. 4a,b). We administered tamoxifen to both neonatal and adult mice (P0 and P30). When we analyzed the brains of neonatal and adult mice 28 days after tamoxifen injection, we observed tdTomato-expressing (tdTomato +) B1-like cells concentrated in the ventral V-SVZ (Fig. 4c–f and 7g). In the OB, we observed many labeled interneurons, including Type 1-4 cells (Fig. 4g–k). These results indicate that at least some Type 1-4 cells originate from SHH-responsive neural stem cells.

We next tested whether SHH activation is sufficient to ectopically specify Type 1-4 cells by injecting Ad:Cre into *SmoM2$^{fl/+}$;Ai14* neonatal mouse brains (Fig. 4l). In these mice, Ad:Cre infected radial glia and their progeny express SmoM2, a constitutively active mediator of Shh signaling[30]. When we targeted NSCs in the dorsal V-SVZ in *Ai14* control animals, we observed tdTomato+ cells in the targeted region of the V-SVZ (Fig. 4m) and primarily superficial GCs and some PGCs in the OB (Fig. 4n). As previously described[27], tdTomato+ GCs derived from SmoM2-expressing NSCs were shifted from superficial to deep (Fig. 4o), confirming that SHH signaling was ectopically activated. However, we did not observe ectopic production of Type 1-4 cells from SmoM2-expressing dorsal progenitors among the tens of thousands of neurons we observed in the OB, indicating that under the conditions we tested, the strong induction of SHH signaling was not sufficient to specify Type 1-4 cells. These results suggest that other factors are required for Type 1-4 cell specification. To identify these factors, we sought to define the borders of the Type 1-4 cell progenitor domains and to test whether TFs expressed within these borders contribute to Type 1-4 cell generation.

Progenitors of Type 1-4 cells do not express Nkx2.1

To molecularly define the borders of Type 1-4 cell progenitor domains, we first tested whether Nkx2.1+ progenitors contribute to Type 1-4 cell production. Nkx2.1 is a compelling candidate TF for Type 1-4 cell specification since it is expressed in the embryonic MGE and vLGE[31–34], and is maintained in late embryonic and early postnatal brains in the ventral tip of the V-SVZ[35,36]. Furthermore, lineage-tracing experiments have shown that Nkx2.1+ cells contribute to OB neurogenesis[12,37]. We first analyzed the spatial extent of Nkx2.1+ cells in neonatal and adult brains by immunofluorescence and observed expression in the ventral tip of the V-SVZ starting at the level of the bed nucleus of the stria terminalis (Bregma +0.6 mm) (Fig. 5d–f and 7h) and extending caudally towards the anterior pretectal nucleus (Bregma −2.0 mm).

Next, we used an inducible *Nkx2.1::CreER;Ai14* system[38] (Fig. 5a) to test whether postnatal *Nkx2.1*+ progenitors give rise to Type 1-4 cells. Since low numbers of OB neurons are derived from adult *Nkx2.1*+ progenitors[12] we induced recombination in newborn *Nkx2.1::CreER^{T2};Ai14* pups with daily injections of tamoxifen from P2–P6 and analyzed their brains 28 days later (Fig. 5b). We observed many labeled cells in the V-SVZ and in the cerebral cortex of tamoxifen-injected animals, indicating efficient Cre-mediated recombination. The labeled cells we observed in the ventral V-SVZ were distributed in a pattern consistent with our immunostaining data (Fig. 5c). The cortical cells we observed might have been labeled by the persistent expression of the CreER^{T2} transgene in

postmitotic cortical interneurons, or they might be derived from the V-SVZ as suggested by a recent study[35]. Although we observed the production of OB GCs and PGCs upon *Nkx2.1::CreER^{T2}* lineage tracing (Fig. 5g,h), we never observed the generation of Type 1-4 cells in tamoxifen-injected mice (n=10). These results suggest that Type 1-4 cells are likely generated in progenitor domains anterior to the broad *Nkx2.1* expression domain.

Nkx6.2^{+} progenitors contribute to Type 1-4 cell generation

Nkx6.2 is another candidate TF that may define specific adult NSC populations. In the embryo, this TF is expressed in two small domains of the telencephalon: the interganglionic sulcus, and the ventral septum[39]. Although its expression in the adult brain has not been described, Nkx6.2 is known to be a SHH-responsive gene and may thus be expressed in the postnatal brain in zones of high SHH activity. To determine whether this is the case and to identify *Nkx6.2*-derived OB neurons, we generated a novel *Nkx6.2::CreER^{T2};Ai14* mouse line to permit *Nkx6.2* lineage tracing. First, we used *in situ* hybridization to confirm that *CreER^{T2}* expression was confined to the *Nkx6.2* expression domain. At E11.5, both *Nkx6.2* and *CreER^{T2}* were expressed in the ventral LGE/dorsal MGE and at E15.5, their expression was confined to the medial and lateral walls of ventral tip of the V-SVZ (Fig. S3). In order to determine if *Nkx6.2*+ adult neural stem cells generate Type 1-4 cells, we administered tamoxifen to reporter mice from P30-34 and analyzed labeled cells at P62 (Fig. 5i,j). Within the adult V-SVZ, we observed a narrow and specific band of reporter gene expression in a region spanning the medial and lateral walls of the very ventral tip of the V-SVZ, extending from Bregma +1.5 mm to approximately Bregma −0.2 mm (Fig. 5k and 7i). In the olfactory bulb, we observed many labeled deep granule cell, as expected (Fig. 5l). Importantly, we also observed many examples of Type 1, 2, 3 and 4 cells (1.8+/−0.4% of all tdTomato+ cells, n=4 mice; Fig. 5m–p). These data support the interpretation that Type 1-4 cells continue to be produced in the adult brain by NSCs in a restricted domain in the anterior ventral V-SVZ.

Zic+ progenitors contribute to a subset of Type 1-4 cells

We next examined additional TFs expressed in the ventral V-SVZ that might contribute to the specification of Type 1-4 cells. We focused on the zinc finger TF of the cerebellum (Zic) family of TFs for several reasons. First, ISH data show that Zic1 and Zic3 are sparsely expressed in the OB in the superficial granule cell layer (GL), mitral cell layer (MCL), and external plexiform layer (EPL), where Type 1-4 cells are located[40]. Second, *Zic1$^{-/-}$;Zic3$^{-/-}$* mice have smaller OBs, suggesting that Zics regulate OB neurogenesis[40]. Third, Zics are highly expressed in the septum (medial wall), but not in other brain regions known to contribute to the V-SVZ[41]. The septum is thought to developmentally contribute to the medial wall of the anterior V-SVZ, a region that may overlap with the progenitor domains for Type 1-4 cells. For these reasons, we hypothesized that progenitors on the medial wall of the anterior ventral V-SVZ and their progeny in the OB might express Zic TFs.

To test this hypothesis, we characterized the Zic expression pattern in the adult OB and V-SVZ with an antibody that specifically recognizes Zic1/2/3[42,43]. The Zic protein expression pattern we observed in the OB was consistent with existing ISH data (Fig. 6d). In the V-SVZ, Zic was expressed near the medial wall of the anterior ventral V-SVZ (Fig. 6a–c, 7b,

and S4). Next, we asked if Zic is expressed in the neurogenic lineage consisting of Type B1 cells (GFAP+ NSCs), transit amplifying Type C cells, and Type A cells (neuroblasts)[44]. To aid in the morphological identification of these cells, we performed this analysis in Z/EG mice injected with Ad:Cre to target the medial or lateral wall of the anterior ventral V-SVZ. We found that Zic expression was barely detectable in a small subset of GFAP-expressing B1-like cells on the medial wall (Fig. 6g), but not on the lateral wall. Zic was clearly detectable in a subset of proliferative (EdU-incorporating and Ki67+) Type C-like cells on the medial wall, but not on the lateral wall (Fig. 6i,j). We also observed Zic in doublecortin- (Dcx) expressing Type A-like cells (Fig. 6h) on the medial wall of the V-SVZ, in the RMS, and in the OB core (Fig. 6k). Together, these results suggest that Zic is upregulated in a subpopulation of Type C and A cells derived from B1-like NSCs located in the medial wall of the anterior ventral V-SVZ. Since Zic is also seen in a subset of OB interneuron types, we hypothesized that Zic might be maintained in at least some medially derived OB interneurons after they are born in the V-SVZ.

To test this hypothesis, we immunostained the OBs of Ad:Cre targeted mice for Zic. About 40% of PGCs produced by NSCs labeled in the medial wall of the anterior ventral V-SVZ were Zic+, whereas almost no PGCs derived from the lateral wall were Zic+. To extend this analysis to PGC subtypes, we co-stained PGCs for Zic and CalR, CalB, or TH, and found that while 39.5+/−2.0% of CalR+ interneurons expressed Zic, only 2.5+/−1.6% of CalB+ and 4.4+/−1.3% of TH+ PGCs were Zic+ (Fig. 6e,f and S5). This finding is consistent with the predominantly medial origin of CalR+ interneurons[9]. When we analyzed the Zic expression pattern of Type 1-4 cells in the OB, we found that almost all Type 1 and Type 3 cells were Zic+, whereas most Type 2 or Type 4 cells were immunonegative for Zic (Fig. 6l–p). Together, these studies identify Zic as a candidate molecular mediator for the specification of medially produced OB interneuron types and suggest that Type 1 and 3 cells might be produced from Zic+ progenitor domains on the medial wall of the anterior ventral V-SVZ. This hypothesis could be addressed in future experiments by lineage tracing with Zic reporter mice.

Distinct microdomains partition the anterior ventral V-SVZ

To better define the borders of Type 1-4 cell progenitor domains and complement our TF-lineage tracing data, we digitally traced spatial extent labeled V-SVZ cells in the 80 injected hemispheres that contained Type 1-4 cells. We then aligned and overlayed these traces onto a common template to identify overlapping V-SVZ regions that consistently gave rise to novel interneurons. This analysis identified a small region comprising the ventral tip (both medial and lateral walls) of the anterior lateral ventricle as a “hot spot” for Type 1-4 cell production (Fig. 7a,b). As expected, this region is rostral to the Nkx2.1 expression domain (Bregma +0.6 to +1.6 mm) but partially overlaps with the Zic expression domain and includes the rostral portion of the Nkx6.2 domain (Fig. 7g–j). When this region was specifically targeted with Ad:Cre, Type 1-4 cells accounted for a substantial fraction (7.4+/−2.9%, n=20 mice) of labeled OB cells.

Next, we hypothesized that Type 1-4 cells are produced in spatially distinct domains. A patch of labeled progenitors has a diameter of about 200 microns, which might span multiple

small progenitor domains. Therefore, we selected the 10 injections that generated the highest percentage of Type 1 cells relative to all other labeled cells in the OB and identified the overlapping regions of labeled progenitors in the V-SVZ in these injections. By repeating this analysis for Type 2–4 cells, we found that Type 1 and Type 3 cells were predominantly generated by radial glia labeled on the medial wall of the anterior ventral V-SVZ. The progenitors of Type 1 cells were restricted to just the very ventral tip of the medial wall (Fig. 7c), whereas Type 3 cells were generated in a medial domain that did not appear to extend down to the tip of the lateral ventricle (Fig. 7e). On the other hand, Type 2 and Type 4 cells were generated in a narrow domain restricted to the ventral tip of lateral V-SVZ (Fig. 7d,f). The spatial origin of Type 1 and 3 cells largely overlapped with the Zic expression domain (Fig. 7j), supporting the hypothesis that Zic contributes to the specification of these cells.

Together, these findings suggest that the four novel interneuron types that we identified are produced in distinct progenitor microdomains in the anterior ventral V-SVZ. These progenitor domains are quite small, extending only about 100–300 μm along the dorsal-ventral axis and 400–800 μm along the rostral-caudal axis (Fig. 7c–f) and collectively covering less than 5% of the surface area of the V-SVZ. Domains of this size would have been almost impossible to discover without a combination of spatially restricted NSC targeting and gene marker analysis, which may explain why the postnatal production of Type 1-4 cells has not been appreciated until now.

DISCUSSION

In this study, we systematically explored the complexity of progenitor domains in the postnatal mouse V-SVZ and identified adult progenitors in the anterior ventral V-SVZ that produce four novel types of OB interneurons. Here, we discuss the unique characteristics of the anterior ventral tip of the V-SVZ, and the possible functional roles of Type 1-4 neurons.

Developmental origin of the anterior ventral V-SVZ

The anterior ventral V-SVZ is located at the junction between the septum and the striatum, two regions that are derived from the embryonic septum and LGE, respectively[34]. The junctions of brain subregions are often sites of overlapping TF codes that specify distinct progenitor identities[8,34]. For example, the border of the LGE and the pallium is a region where pallial TFs such as Emx1 and Pax6 overlap with subpallial TFs such as Dlx1/2/5, Gsx1/2 (Gsh1/2) and Ascl1 (Mash1). This region of overlap defines the spatially limited domain where the TFs Sp8 and Dbx1 are expressed[12,34,45]. Similarly, the overlap of LGE TFs with the septal Zic TFs may define the Nkx6.2 positive progenitor domain in which Type 1-4 cells are produced in the postnatal brain. Notably, Sp8 is also expressed in the septum[46], where it may contribute to the generation of CalR+ Type 1-4 cells.

The lineage relationship between OB neurons originating from common progenitor domains has not been described. For example, within the anterior ventral V-SVZ we observed the production of Type 1 and 3 cells on the medial wall and Type 2 and 4 cells on the lateral wall (Fig. 7). Similarly, superficial GCs and TH+ PGCs are both produced in the dorsal/cortical V-SVZ, and deep GCs and CalB+ PGCs are both produced in the ventral V-SVZ[9]. Therefore, progenitor domains generate different cell types. Whether these are generated by

distinct progenitors with similar developmental histories, or from common progenitors is unknown. This important problem could be addressed by clonal lineage tracing *in vivo*, where the potential of individual NSCs can be assessed.

Potential roles of novel interneurons in the OB circuitry

The continual addition and putative turnover of Type 1-4 cells suggests that these cells are likely to play important functional roles in the OB. Based on their morphological properties and the existing literature, we hypothesize how these four cell types may contribute to the function of the OB:

The dendritic branches of deep-projecting GCs (Type 1) in the granule cell layer and IPL, position these cells to receive input from the axons of mitral and tufted cells and to inhibit the activity of projection neurons above them via their dendrites in the MCL and EPL. Shrub granule cells (Type 2) have spatially restricted, bushy arbors decorated with many spines that are concentrated near the proximal dendrites and cell bodies of mitral and tufted cells. The location of synapses on these cells close to the cell bodies of OB projection neurons suggests that these cells may mediate lateral inhibition. The extensive processes of PMCs (Type 3) in the MCL and IPL suggest that they may interact with the cell bodies and axonal collaterals of mitral and tufted cells. The long, varicose processes of satellite cells have previously been shown to associate with the dendrites of OB projection neurons, positioning them to inhibit broad stretches of mitral and tufted cell dendrites. A schematic diagram of Type 1-4 cells in relation to other OB cell types is given in Fig. S6.

While the functions of G_{IV}, G_V, PMC and SC (Type 1-4) cells are unclear, all of these cell types are generated postnatally, almost doubling the catalog of cell types known to be replaced in the adult brain. Furthermore, we determined that the spatial origin of these cells is restricted to a small region of the anterior ventral V-SVZ that is subdivided into progenitor microdomains at an unexpectedly fine level of organization, correlating well with the expression domains of Zic and Nkx6.2 TFs. This work extends the list of cell types replaced in the postnatal brain and shows how interneuron diversity is achieved by the subdivision of the V-SVZ into distinct progenitor microdomains.

MATERIALS AND METHODS

Neural stem cell targeting

Neural stem cells (NSCs) were targeted by injection of Cre-expressing adenovirus (Ad:Cre or Ad:GFAP-Cre) into Z/EG reporter mice as previously described[9]. All protocols and procedures followed the guidelines of the Laboratory Animal Resource Center at the University of California, San Francisco.

Perfusion and immunohistochemistry

Mice were sacrificed and their brains were processed for immunohistochemistry as previously described[9]. Antibodies used are given in Table S1. Biotin-conjugated antibodies were visualized by ABC reaction (Vector) followed by diaminobenzidine (DAB) with or without nickel.

Generation of Nkx6.2-CreERT2 transgenic mice

Mice expressing CreER^{T2} under control of the Nkx6.2 gene were generated using bacterial artificial chromosome (BAC) transgenic technology as previously described[47]. A codon-improved iCreER^{T2} recombinase was fused to the initiation codon of the Nkx6.2 gene using a PCR-based approach. A simian virus 40 polyadenylation signal was inserted at a position immediately after the ATG-encoding exon of Nkx6.2 (Fig. S3). BAC modification was performed in a bacterial system as described previously[48].

Identification and region of origin analysis of novel cell types

To determine the V-SVZ regions where these cell types were produced, we traced coronal brain sections from the Allen Brain Reference Atlas (http://mouse.brain-map.org/atlas/ARA/Coronal/browser.html) in Adobe Illustrator CS (Adobe Systems Inc.) at approximately 200 μm increments from the OB (coronal level 26, Bregma 4.845 mm) to Bregma (coronal level 54, Bregma 0.020 mm). Next, we digitally painted the V-SVZ regions containing labeled progenitors onto these traces and overlaid them in Illustrator. We selected the 10 hemispheres with the largest percentage of Type 1 cells relative to other labeled OB cell types (Fig. 7c) and overlayed the traces of labeled V-SVZ cells (red) to identify regions in which at least half (5/10) of the traces overlapped (dotted line), to identify likely progenitor domains for each cell type. This analysis was repeated for Type 2-4 cells (Fig. 7d–f), indicating that the progenitor domains of Type 1-4 cells are largely distinct subregions of the anterior ventral V-SVZ.

Imaging and camera lucida tracing

DAB-labeled cells were studied on an Olympus AX70 microscope with a Retiga 2000R digital camera (Qimaging Corporation) and processed using Openlab 5.0.1 (Improvision Inc.). Fluorescent images of immunostained brain sections were taken on a Leica TCS SP5 confocal microscope using the Leica LAS AF imaging software. Images were processed for brightness and contrast using Adobe Photoshop CS (Adobe Systems Inc.). We manually quantified double-labeled cells at 40–100x magnification on an Olympus AX70 microscope. For marker gene analysis, we counted a minimum of 30 different Type 1-4 cells from at least three separate injections. For camera lucida tracing, we selected at least 10 representative DAB-immunostained Type 1-4 cells that had largely intact dendritic arbors with a mature morphology (branched and spine-bearing). We traced only cells that were physically separated from other labeled cells. In Fig. S4, brain sections and GFP+-cells were mapped using Neurolucida® (v10.54 MBF Biosciences-MicroBrightField Inc.).

Morphological analysis

For morphological analysis, at least 20 immunoperoxidase labeled cells of each type (Type 1-4) were studied using ImageJ software (NIH). To calculate the position of the cell in the OB, we measured its radial distance from the center of the MCL and divided this measurement by the radial distance from the OB core to the top of the EPL (bottom of the GL). Similarly, we measured the distance from the center of the MCL to the tip of the most superficial dendrite for each cell type and normalized this distance to the thickness of the EPL. To quantify dendritic branching, the primary dendrite was defined as the longest and

largest diameter neurite emanating from the soma. Secondary dendrites were defined as processes that radiated from this primary dendrite, and tertiary dendrites as processes directly connected to secondary dendrites.

Supplementary Material

Refer to Web version on PubMed Central for supplementary material.

Acknowledgments

We would like to thank Thuhien Nguyen, Zaman Mirzadeh and Rebecca Ihrie helpful comments and discussions that improved this study, and David Rowitch and Rosalind Segal for generously sharing antibodies. Ricardo Romero provided outstanding technical assistance with histology. Matthew Grist, Ulla Dennehy and Michael Humphreys generated the *Nkx6.2::CreER*^{T2} transgenic mice and *Gli1::CreER*^{T2} mice were generously provided by Alexandra Joyner. F.T.M. was supported by the NSF, the Jane Coffin Childs Memorial Fund, the NIH, and the Harvard Stem Cell Institute. L.C.F. is a Howard Hughes Medical Institute fellow of the Helen Hay Whitney Foundation. This study was supported by grants from the NIH (HD 32116 and NS 28478), the John G. Bowes Research Fund, the European Research Council (207807), and the UK Medical Research Council (86419).

References

1. Alvarez-Buylla A, Garcia-Verdugo JM. Neurogenesis in adult subventricular zone. Journal of Neuroscience. 2002; 22:629–634. [PubMed: 11826091]
2. Sakamoto M, et al. Continuous neurogenesis in the adult forebrain is required for innate olfactory responses. Proceedings of the National Academy of Sciences. 2011; 108:8479–8484.
3. Imayoshi I, et al. Roles of continuous neurogenesis in the structural and functional integrity of the adult forebrain. Nature Neuroscience. 2008; 11:1153–1161.
4. Kosaka K, et al. Chemically defined neuron groups and their subpopulations in the glomerular layer of the rat main olfactory bulb. Neurosci Res. 1995; 23:73–88. [PubMed: 7501303]
5. Price JL, Powell TP. The mitral and short axon cells of the olfactory bulb. J Cell Sci. 1970; 7:631–651. [PubMed: 5492279]
6. Shepherd, GM. The Synaptic Organization of the Brain. Oxford University Press; 2004.
7. Doetsch F, Caille I, Lim DA, Garcia-Verdugo JM, Alvarez-Buylla A. Subventricular Zone Astrocytes Are Neural Stem Cells in the Adult mammalian Brain. Cell. 1999; 97:703–716. [PubMed: 10380923]
8. Alvarez-Buylla A, Kohwi M, Nguyen TM, Merkle FT. The Heterogeneity of Adult Neural Stem Cells and the Emerging Complexity of Their Niche. Cold Spring Harbor Symposia on Quantitative Biology. 2008; 73:357–365.
9. Merkle FT, Mirzadeh Z, Alvarez-Buylla A. Mosaic Organization of Neural Stem Cells in the Adult Brain. Science. 2007; 317:381–384. [PubMed: 17615304]
10. Kelsch W, Mosley CP, Lin CW, Lois C. Distinct Mammalian Precursors Are Committed to Generate Neurons with Defined Dendritic Projection Patterns. PLoS Biol. 2007; 5:e300. [PubMed: 18001150]
11. Ventura RE, Goldman JE. Dorsal Radial Glia Generate Olfactory Bulb Interneurons in the Postnatal Murine Brain. Journal of Neuroscience. 2007; 27:4297–4302. [PubMed: 17442813]
12. Young KM, Fogarty M, Kessaris N, Richardson WD. Subventricular Zone Stem Cells Are Heterogeneous with Respect to Their Embryonic Origins and Neurogenic Fates in the Adult Olfactory Bulb. Journal of Neuroscience. 2007; 27:8286–8296. [PubMed: 17670975]
13. Kriegstein A, Alvarez-Buylla A. The Glial Nature of Embryonic and Adult Neural Stem Cells. Annu Rev Neurosci. 2009; 32:149–184. [PubMed: 19555289]
14. Novak A, Guo C, Yang W, Nagy A, Lobe CG. Z/EG, a double reporter mouse line that expresses enhanced green fluorescent protein upon Cre-mediated excision. genesis. 2000; 28:147–155. [PubMed: 11105057]

15. Seri B, et al. Composition and organization of the SCZ: a large germinal layer containing neural stem cells in the adult mammalian brain. Cereb Cortex. 2006; 16 (Suppl 1):i103–11. [PubMed: 16766696]
16. Kohwi M, et al. A subpopulation of olfactory bulb GABAergic interneurons is derived from Emx1- and Dlx5/6-expressing progenitors. J Neurosci. 2007; 27:6878–6891. [PubMed: 17596436]
17. Alonso M, et al. Turning Astrocytes from the Rostral Migratory Stream into Neurons: A Role for the Olfactory Sensory Organ. Journal of Neuroscience. 2008; 28:11089–11102. [PubMed: 18945916]
18. Mirzadeh Z, Merkle FT, Soriano-Navarro M, Garcia-Verdugo JM, Alvarez-Buylla A. Neural Stem Cells Confer Unique Pinwheel Architecture to the Ventricular Surface in Neurogenic Regions of the Adult Brain. Cell Stem Cell. 2008; 3:265–278. [PubMed: 18786414]
19. SHEPHERD G, CHEN W, WILLHITE D, MIGLIORE M, GREER C. The olfactory granule cell: From classical enigma to central role in olfactory processing. Brain Research Reviews. 2007; 55:373–382. [PubMed: 17434592]
20. Schneider SP, Macrides F. Laminar Distributions of Interneurons in Main Olfactory-Bulb of Adult Hamster. Brain Research Bulletin. 1978; 3:73–82. [PubMed: 630423]
21. Mori K, Kishi K, Ojima H. Distribution of Dendrites of Mitral, Displaced Mitral, Tufted, and Granule Cells in the Rabbit Olfactory-Bulb. The Journal of comparative neurology. 1983; 219:339–355. [PubMed: 6619342]
22. Blanes T. Sobre algunos puntos dudosos de la estrucutra del bulbo olfactario. Revta trimest Microgr. 1898; 3:99–127.
23. Shepherd GM. Synaptic organization of the mammalian olfactory bulb. Physiol Rev. 1972; 52:864–917. [PubMed: 4343762]
24. López-Mascaraque L, De Carlos JA, Valverde F. Structure of the olfactory bulb of the hedgehog (Erinaceus europaeus): a Golgi study of the intrinsic organization of the superficial layers. J Comp Neurol. 1990; 301:243–261. [PubMed: 2262591]
25. Larriva-Sahd J. The accessory olfactory bulb in the adult rat: a cytological study of its cell types, neuropil, neuronal modules, and interactions with the main olfactory system. J Comp Neurol. 2008; 510:309–350. [PubMed: 18634021]
26. Van Gehuchten A IM. Le bulbe olfactif chez quelques mammiferes. La Cellule. 1891; 5:205–237.
27. Ihrie RA, et al. Persistent Sonic Hedgehog Signaling in Adult Brain Determines Neural Stem Cell Positional Identity. Neuron. 2011; 71:250–262. [PubMed: 21791285]
28. Ahn S, Joyner AL. Dynamic changes in the response of cells to positive hedgehog signaling during mouse limb patterning. Cell. 2004; 118:505–516. [PubMed: 15315762]
29. Danielian PS, Muccino D, Rowitch DH, Michael SK, McMahon AP. Modification of gene activity in mouse embryos in utero by a tamoxifen-inducible form of Cre recombinase. Current Biology. 1998; 8:1323–1326. [PubMed: 9843687]
30. Mao J, et al. A novel somatic mouse model to survey tumorigenic potential applied to the Hedgehog pathway. Cancer research. 2006; 66:10171–10178. [PubMed: 17047082]
31. Price M. Members of the Dlx- and Nkx2-gene families are regionally expressed in the developing forebrain. J Neurobiol. 1993; 24:1385–1399. [PubMed: 7901324]
32. Sussel L, Marin O, Kimura S, Rubenstein JL. Loss of Nkx2.1 homeobox gene function results in a ventral to dorsal molecular respecification within the basal telencephalon: evidence for a transformation of the pallidum into the striatum. Development. 1999; 126:3359–3370. [PubMed: 10393115]
33. Marin O, Anderson SA, Rubenstein JL. Origin and molecular specification of striatal interneurons. J Neurosci. 2000; 20:6063–6076. [PubMed: 10934256]
34. Flames N, et al. Delineation of Multiple Subpallial Progenitor Domains by the Combinatorial Expression of Transcriptional Codes. Journal of Neuroscience. 2007; 27:9682–9695. [PubMed: 17804629]
35. Taniguchi H, Lu J, Huang ZJ. The Spatial and Temporal Origin of Chandelier Cells in Mouse Neocortex. Science. 2013; 339:70–74. [PubMed: 23180771]

36. Magno L, Catanzariti V, Nitsch R, Krude H, Naumann T. Ongoing expression of Nkx2.1 in the postnatal mouse forebrain: potential for understanding NKX2.1 haploinsufficiency in humans? Brain Research. 2009; 1304:164–186. [PubMed: 19766601]
37. Xu Q, Tam M, Anderson SA. Fate mapping Nkx2.1-lineage cells in the mouse telencephalon. J Comp Neurol. 2008; 506:16–29. [PubMed: 17990269]
38. Tsai H-H, et al. Regional Astrocyte Allocation Regulates CNS Synaptogenesis and Repair. Science. 201210.1126/science.1222381
39. Moreno-Bravo JA, Perez-Balaguer A, Martinez S, Puelles E. Dynamic expression patterns of Nkx6.1 and Nkx6.2 in the developing mes-diencephalic basal plate. Dev Dyn. 2010; 239:2094–2101. [PubMed: 20549744]
40. Inoue T, Ota M, Ogawa M, Mikoshiba K, Aruga J. Zic1 and Zic3 Regulate Medial Forebrain Development through Expansion of Neuronal Progenitors. Journal of Neuroscience. 2007; 27:5461–5473. [PubMed: 17507568]
41. Aruga J, et al. A novel zinc finger protein, zic, is involved in neurogenesis, especially in the cell lineage of cerebellar granule cells. J Neurochem. 1994; 63:1880–1890. [PubMed: 7931345]
42. Wataya T, et al. Minimization of exogenous signals in ES cell culture induces rostral hypothalamic differentiation. Proceedings of the National Academy of Sciences. 2008; 105:11796–11801.
43. Borghesani PR, et al. BDNF stimulates migration of cerebellar granule cells. Development. 2002; 129:1435–1442. [PubMed: 11880352]
44. Doetsch F, Garcia-Verdugo JM, Alvarez-Buylla A. Cellular composition and three-dimensional organization of the subventricular germinal zone in the adult mammalian brain. J Neurosci. 1997; 17:5046–5061. [PubMed: 9185542]
45. Puelles L, et al. Pallial and subpallial derivatives in the embryonic chick and mouse telencephalon, traced by the expression of the genes Dlx-2, Emx-1, Nkx-2.1, Pax-6, and Tbr-1. J Comp Neurol. 2000; 424:409–438. [PubMed: 10906711]
46. Waclaw RR, et al. The Zinc Finger Transcription Factor Sp8 Regulates the Generation and Diversity of Olfactory Bulb Interneurons. Neuron. 2006; 49:503–516. [PubMed: 16476661]
47. Fogarty M, et al. Spatial genetic patterning of the embryonic neuroepithelium generates GABAergic interneuron diversity in the adult cortex. Journal of Neuroscience. 2007; 27:10935–10946. [PubMed: 17928435]
48. Lee EC, et al. A highly efficient Escherichia coli-based chromosome engineering system adapted for recombinogenic targeting and subcloning of BAC DNA. Genomics. 2001; 73:56–65. [PubMed: 11352566]

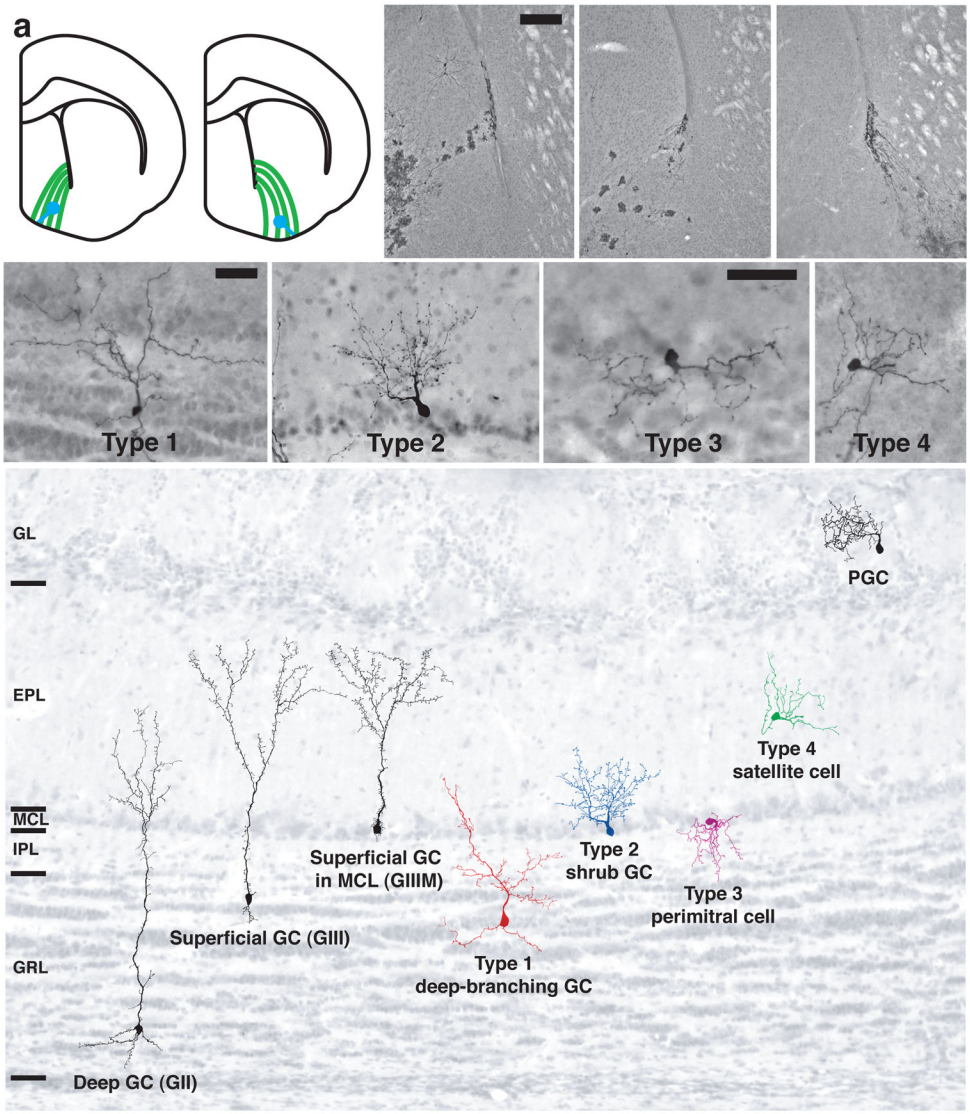

Figure 1. Production of novel OB cell types by specifically labeled NSCs

a) Schematic diagram of radial glial cell targeting. Stereotaxic injections of small volumes of adenovirus infect cells locally at the injection site and needle tract (blue) as well as the long basal processes of radial glia (green), which transform into adult NSCs. **b–d)** DAB-stained photomicrographs of labeled cells in the P28 brain on the medial (**b,c**) and lateral (**d**) walls of the lateral ventricle. **e–h**) Labeled NSCs in this region of the V-SVZ generated novel labeled OB cell types (Type 1-4), stained here by DAB. **i)** Schematic diagram showing camera lucida traces of known adult-born OB interneurons (black) and novel cell types (red, blue, magenta, green) superimposed over a photomicrograph of a hematoxylin-stained OB to show their relative positions. Cells are shown to scale, and the pial surface is up. Scale bars are 75 μm for b–d and 25 μm for E-H. EPL, external plexiform layer; GC, granule cell; GL, glomerular layer; GRL, granule cell layer, IPL, internal plexiform layer; MCL, mitral cell layer; PCG, periglomerular cell.

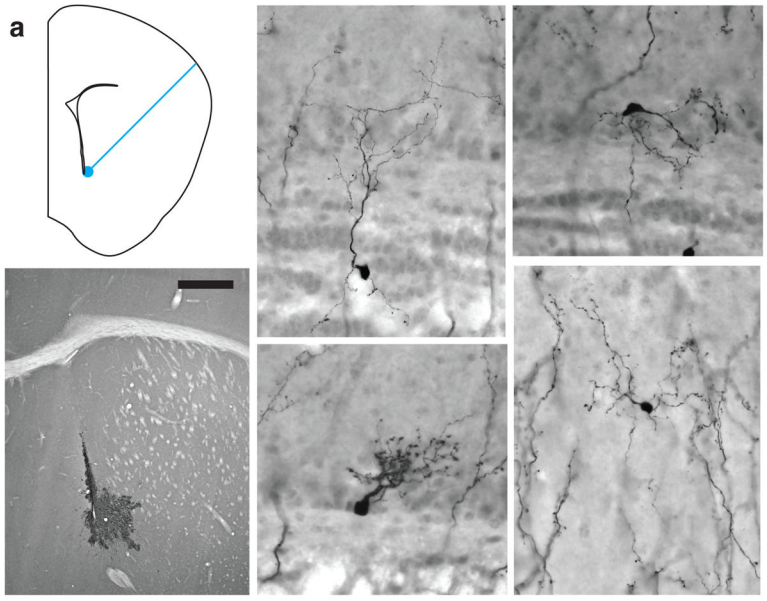

Figure 2. Type 1-4 cells continue to be produced by GFAP+ NSCs in the adult anterior ventral V-SVZ

a) Diagram showing the injection tract (blue line) and injection site (blue circle) of Ad:GFAP-Cre targeting the anterior-ventral V-SVZ in a coronal schematic diagram of the adult (P60) brain hemisphere (midline to the left, dorsal is up). **b)** DAB-stained photomicrograph of targeted V-SVZ and labeled striatal astrocytes 28 days after Ad:GFAP-cre injection. **c–f)** Type 1-4 cells can be clearly identified by their distinctive morphology in the OB 28 days after adult neural stem cell labeling. Scale bar is 150 μm for B, 42 μm for c and f, and 25 μm for d and e.

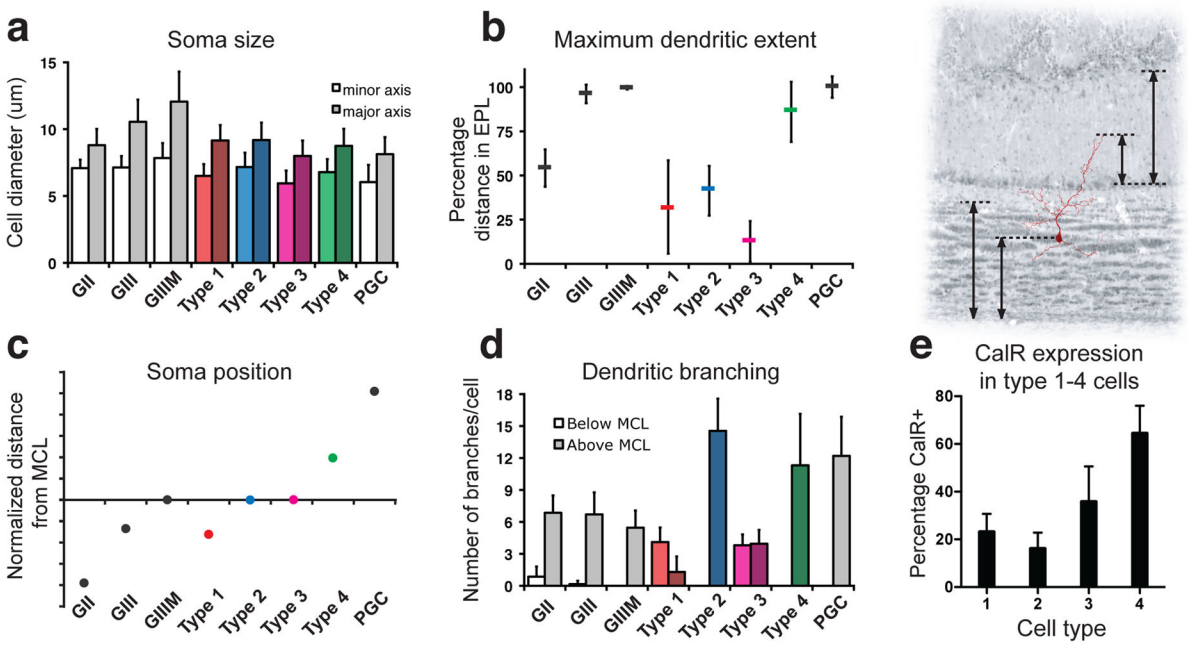

Figure 3. Molecular and morphological characterization of Type 1-4 cells

a) Cell body diameters measured along the minor and major axes are shown for Type 1-4 cells alongside granule and periglomerular cells. **b)** Quantification of soma position in the OB relative to the MCL normalized to the thickness of the GRL and EPL. **c)** Maximum reach of the dendritic arbor into the EPL for each cell type. Note that although Type 1 and 2 cells had superficially located cell bodies, their dendrites were restricted to the lower EPL, whereas superficial granule cells (G_{III}, $G_{III}M$) consistently reached the most superficial EPL. **d)** Analysis of the number of secondary and tertiary branches extending from the primary dendrite reveals a unique branching pattern that, along with other morphological characteristics, distinguishes Type 1-4 cells from granule and periglomerular cells. **e)** A subset of Type 1-4 cells expressed CalR. Data are expressed as mean±s.d. for a–d and mean ±s.e.m for e. At least five mice were examined in each experimental group. Abbreviations for cell types and OB regions are given in Figure 1. CalR, calretinin.

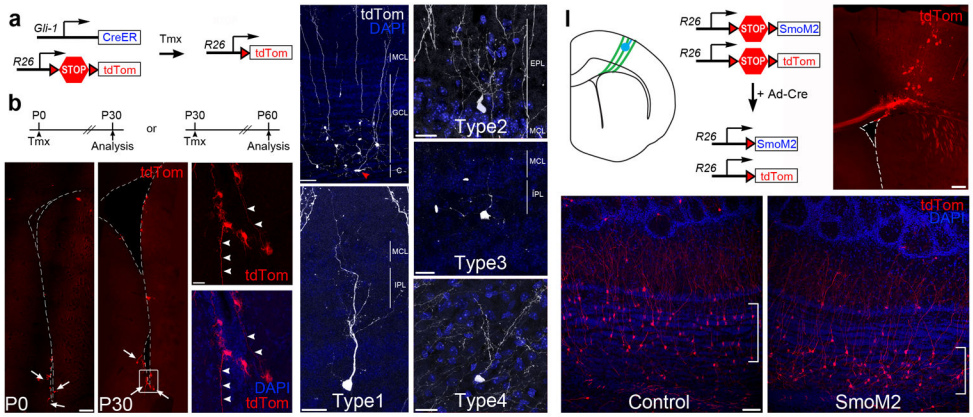

Figure 4. Type 1-4 cells are produced by Gli1-expressing progenitors

a) Diagram showing the *Gli1-CreER*^{T2} and *Rosa26-Ai14* alleles. **b)** *Gli1::CreER*^{T2}*;R26R-Ai14* neonates (P0) and adult (P30) mice were treated with tamoxifen and analyzed 30 days later. **c–f)** The majority of *Gli1*-expressing progenitors are located in the ventral V-SVZ in P0 (c) or P30 (d) animals (arrows) and frequently have B1 cell-like morphology with long basal processes (arrowheads, e). **g)** *Gli1*+-progenitors generate mainly deep GCs located close to the core of the OB. Arrowhead (red) denotes a migrating neuroblast in the OB core (c, core). **h–k)** Type 1-4 cells are produced by *Gli1*-expressing progenitors. In this image, the tdTomato staining has been pseudocolored to improve its contrast. These are representative examples of type 1-4 observed from n=13 mice. **l)** Schematic diagram showing the targeting of radial glia (green) in the cortical V-SVZ with Ad:Cre (blue) of a neonatal (P0) *R26R-LSL-SmoM2;R26R-Ai14* mouse brain. Upon Cre recombination, a constitutive active form of the Smo receptor (SmoM2) and tdTomato are expressed in cortical radial glia and their progeny. **m)** Photomicrograph of a targeted *R26R-Ai14* brain section 28 days after Ad:Cre injection. **n–o)** Cortical Ad:Cre injections in control *R26R-Ai14* neonates generated mostly superficial GCs (in brackets, m), while *SmoM2;R26R-Ai14* neonates produced deep granule cells (in brackets, n), but no Type 1-4 cells. These images are representative for each genotype of at least three independent experiments. Scale bar is 120 μm for c, 20 μm for e–j, 200 μm for l, and 60 μm for e.

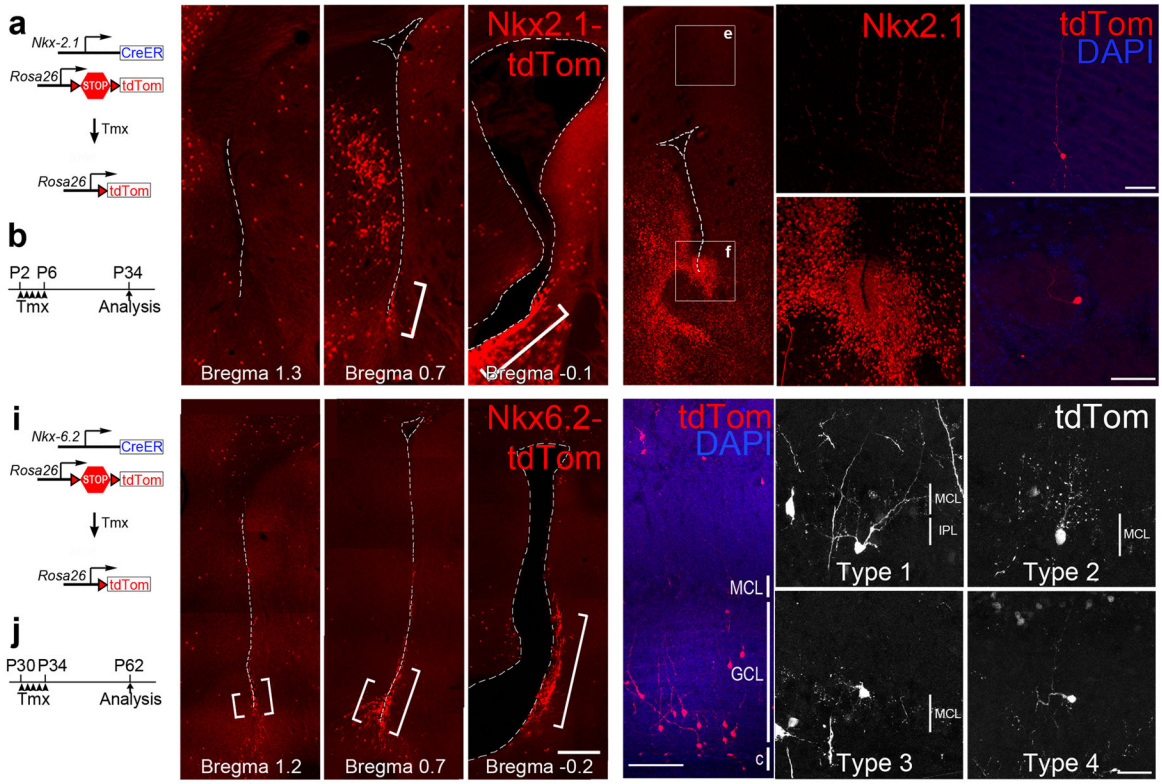

Figure 5. Type 1-4 cells are produced by postnatal progenitors expressing Nkx6.2, but not in Nkx2.1

a,b) Diagram showing the *Nkx2.1::CreER*^{T2} and *Rosa26-Ai14* alleles (a) and timing of tamoxifen (Tmx) administration and analysis (b) **c)** *Nkx2.1* lineage-traced (tdTomato-expressing) cells are present in the ventral V-SVZ (brackets), shown here in coronal sections at different caudal-rostral levels**. d–f)** Immunofluorescence for Nkx2.1 protein in the neonatal mouse brain showing strong Nkx2.1 expression in the ventral V-SVZ (near the bed nucleus of the stria terminalis in d and f) but no expression in the cortex (d and e). **g–h)** *Nkx2.1*-expressing progenitors generate granule (g) and periglomerular (h) cells but not Type 1-4 cells. **i,j)** Diagram showing the *Nkx6.2::CreER*^{T2} and *Rosa26-Ai14* alleles (i) and timing of Tmx administration and analysis (j). **k)** *Nkx6.2* lineage-traced cells with B1 cell-like morphology are present in the anterior ventral V-SVZ (brackets). **l)** *Nkx6.2*+-progenitors generate mainly deep GCs located close to the core of the OB. **m–p)** Type 1-4 cells are produced by *Nkx6.2*-expressing progenitors. In this image, the tdTomato staining has been pseudocolored to improve its contrast. Scale bar is 60 μm for g–h, 200 μm for k–l, and 25 μm for m–p.

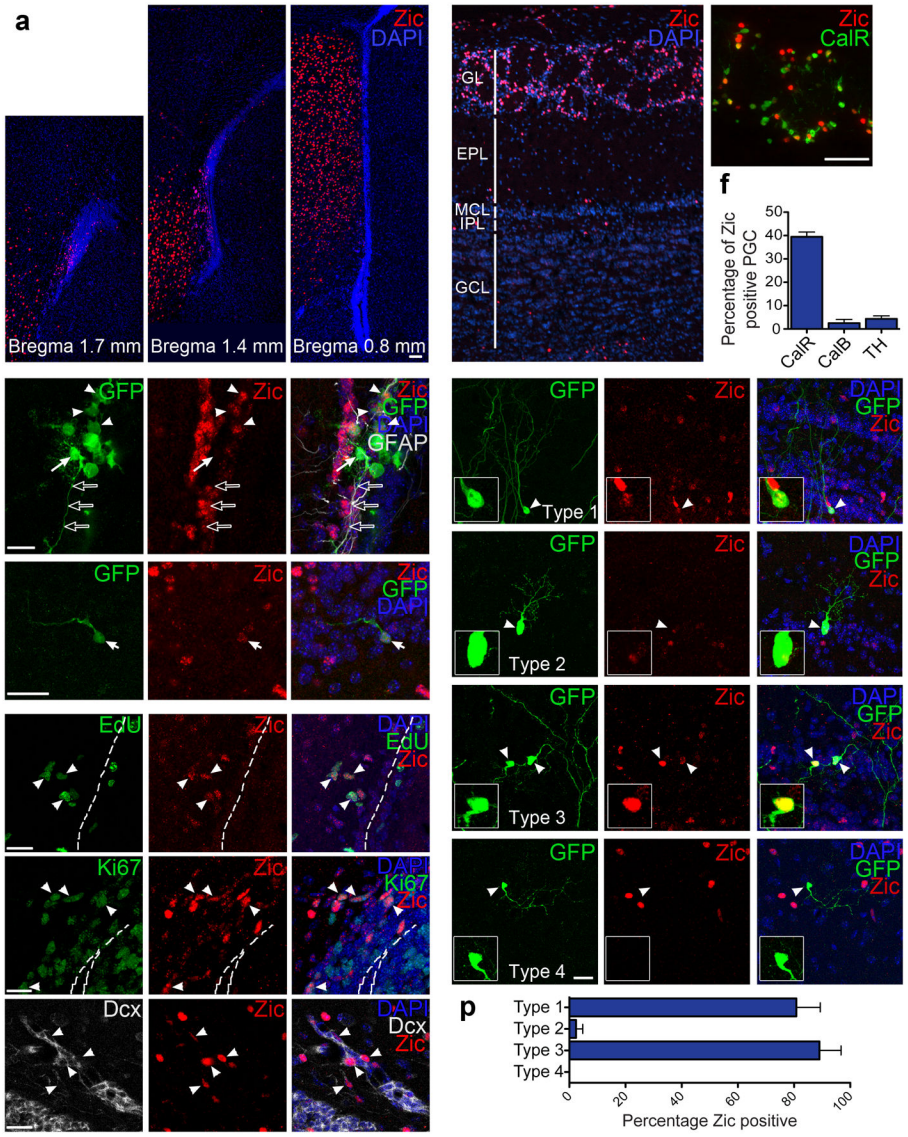

Figure 6. Zic1/2/3 expression partitions Type 1-4 production domains

a–c) Photomicrographs of coronal adult brain sections at three rostrocaudal levels showing Zic immunopositive cells in the medial wall of the adult V-SVZ. **d)** Zic expression in the OB, including the glomerular layer (GL), external plexiform layer (EPL), mitral cells layer (MCL), internal plexiform layer (IPL), and superficial granule cell layer (GCL). **e)** Co-localization of Zic and the OB interneuronal marker calretinin (CalR). Data are expressed as mean±s.e.m. At least three mice per group were examined. **f)** Quantification of CalR, CalB and TH expression in Zic+ periglomerular cells. **g–h)** Zic expression in GFP-positive V-SVZ cell types derived from Ad:Cre targeted radial glia in the medial V-SVZ. Zic is barely detectable in a small subpopulation of GFAP+ B1 cells (closed arrow, B1 cell body; open arrows, basal process, in **g**). Zic is expressed in cells with morphologies characteristics of transit-amplifying cells (arrowheads in g) and migrating neuroblasts (in the RMS) (arrow in h). **i–j)** Zic+ proliferating progenitors in the medial V-SVZ incorporate EdU (1 hr survival) (i), and express Ki67 (j). **k)** Within chains of migrating neuroblasts, Zic is expressed by a

subpopulation of doublecortin (Dcx)+ neuroblasts (arrowheads). **l–o)** The majority of Type 1 (l) and Type 3 (n) cells express Zic protein, while Type 2 (m) and Type 4 (o) cells are mostly Zic negative. **p**) Quantification of Zic expression in Type 1-4 cells. Data are presented as mean±s.e.m., n=13 mice. Scale bar is 60 μm for a–c, and e and 20 μm for g–o.

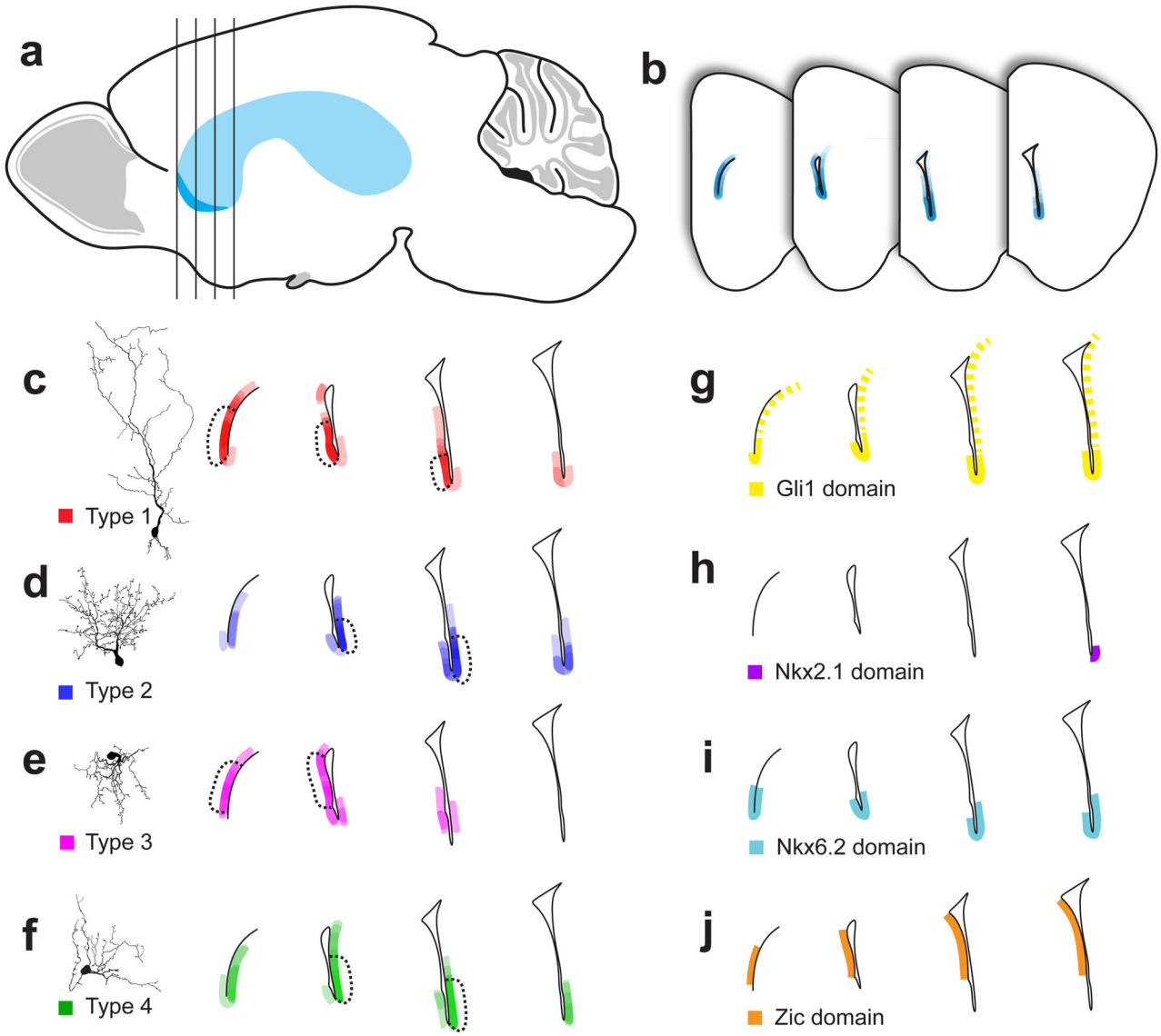

Figure 7. Type 1-4 cells are produced in distinct subregions of the anterior ventral V-SVZ

a) Schematic lateral view of an adult mouse brain indicating the approximate spatial extent of the V-SVZ (light blue) including the subdomains that give rise to Type 1-4 cells (darker blue). Vertical lines indicate the approximate regions from which the outline of the lateral ventricle is shown in coronal section in (b–f). **b)** Labeled V-SVZ regions (blue) of brains containing labeled Type 1-4 cells were traced and overlaid onto a common template to reveal the origin of Type 1-4 cells (darker blue). **c–f)** This analysis was repeated for those brain regions giving rise to the highest percentage of Type 1, 2, 3, or 4 cells, revealing a unique spatial origin for each of these cell types. **g–i)** Approximate spatial extent of the *Gli1* (g) and *Nkx2.1* (h), and *Nkx6.2* (i) expression domains, based on $CreER^{T2}$ lineage tracing. Dashed line in (g) indicates lower expression. Nkx2.1 data in (h) are supported by immunostaining. **j)** Approximate spatial extent of the Zic1/2/3 expression domain based on immunostaining (see also Fig. 6 and S4).